Oil Ganglion Dynamics During Immiscible Displacement: Model Formulation

A. C. PAYATAKES
K. M. NG
and
R. W. FLUMERFELT

Chemical Engineering Department
University of Houston
Houston, Texas 77004

A model is formulated in order to study the transient behavior of oil ganglion populations during immiscible displacement in oil recovery processes. The model is composed of three components: a suitable model for granular porous media; a stochastic simulation method capable of predicting the expected fate (mobilization, breakup, stranding) of solitary oil ganglia moving through granular porous media; and two coupled ganglion population balance equations, one applying to moving ganglia and the other to stranded ones. The porous medium model consists of a regular network of randomly sized unit cells of the constricted tube type. Based on this model and a mobilization-breakup criterion, computer aided simulations provide probabilistic information concerning the fate of solitary oil ganglia. Such information is required in the ganglion population balance equations, the solution of which delineates the conditions under which oil bank formation succeeds or fails. Successful oil bank formation depends on the outcome of the competition between the process of oil ganglion deterioration through breakup and stranding on one hand and the process of oil ganglion collision and coalescence on the other. The parameters entering the system of population balances are initial ganglion number concentration, average ganglion velocity, ganglion dispersion coefficients, ganglion stranding coefficient, ganglion breakup coefficient and probability of coalescence given a collision. These parameters are, in turn, functions of the porous medium geometry, capillary number, ganglion size distribution, flood velocity, oil saturation and flood composition.

SCOPE

Even though considerable effort has been devoted by several investigators to the study of the conditions under which a single oil ganglion can get mobilized, no attempt has been made, prior to the present work, to describe theoretically the fate of an oil ganglion, once mobilized. However, the fate of a mobilized oil ganglion and, more importantly, the collective fate of a population of oil ganglia engulfed by a chemical flood are problems of fundamental significance in understanding the formation of an oil bank and elucidating the mechanisms through which significant amounts of oil remain entrapped. A related problem of even higher significance is the shedding of large oil blobs from the trailing edge of a moving oil bank.* Such blobs find themselves immersed in a deteriorated and probably incompetent part of the chemical flood, and as they move they continue breaking down into smaller ganglia which gradually get stranded. Hence, a flood fails to mobilize all the oil in place; moreover, a significant part of the mobilized oil is left behind by the moving oil bank in the form of a trail of stranded ganglia.

Clearly, in order to develop a good understanding of the dynamics of these phenomena, formulation of a realistic porous medium model, which can be used for the study of oil ganglion motion, coalescence, breakup and stranding is necessary.

The need for such a porous medium model has been stressed repeatedly by several investigators. Melrose (1970) points out that in order to predict the set of experimental observations usually recorded, knowledge of the cooperative behavior of an ensemble of a very large number of interconnected cavities is required. Various models for investigating the statistical aspects of immiscible displacement have been proposed in the past (Fatt, 1956; Everett, 1958; Ksenzhek, 1963; Iczkowski, 1968) but have not succeeded in incorporating all the necessary features of the porous medium. A comprehensive review of porous medium models with special reference to their applicability to the modeling of drainage and imbibition was given by van Brakel (1975), who concluded that none of the porous medium models existing at that time succeeded in providing a satisfactory basis for the modeling or simulation of immiscible displacement.

The objectives of the present line of investigation are: the development of a suitable porous medium model for unconsolidated granular media, the theoretical and experimental study of the fate of solitary ganglia and the development of a method for the quantitative prediction of the dynamics of large populations of oil ganglia in porous media of this type. It is hoped that the results will provide useful insights that can be transferred to real reservoirs. It is also conceivable that the method can be generalized sufficiently to allow quantitative studies in consolidated porous media.

CONCLUSIONS AND SIGNIFICANCE

A model for unconsolidated packings of grains or spheres is developed which is suitable for the modeling of the dynamics of oil ganglia during immiscible displacement. This model consists of a network of randomly sized unit cells of the constricted tube type.

A mobilization-breakup criterion is formulated in a companion publication (Ng and Payatakes, 1980) which takes into account the size, shape and orientation of the oil ganglion; the local topology of the porous medium; the interfacial tension; the wettability and the macroscopic pressure gradient. Based on this criterion a computer-aided stochastic simulation method is developed for the prediction of the fate of solitary oil ganglia. As an illustration, the probabilities of mobilization, breakup and stranding per rheon, the stranding coefficient and the breakup coefficient are calculated under typical conditions (a more extensive study is given in Ng and Payatakes, 1979). One of the major conclusions arising from these simulations is that the probability of breakup per step (rheon) taken by a ganglion is quite high (typically 0.10 to 0.15). Hence, solitary ganglia are destined to disintegrate rapidly into smaller daugh-

*The authors thank Dr. R. L. Reed of Exxon Production Research, Houston, for very helpful discussions on this subject.

0001-1541-80-3681-0430-$01.55

ter ganglia, all of which eventually become stranded (unless the capillary number is high enough, $N_{Ca} > 10^{-2}$, to mobilize small oil ganglia, each occupying just one chamber of the porous medium.).

Two coupled integrodifferential equations [Equations (31) and (32)] are formulated in order to describe the transient behavior of a large population of interacting oil ganglia undergoing immiscible displacement. Expressions for the collision-coalescence kernels of these equations are developed, Equations (34) to (39). Most of the parameters appearing in the population balances, such as the breakup and stranding coefficients, can be calculated readily from the results of the stochastic simulation of the fate of solitary ganglia, Equations (40) and (41). However, two key parameters, namely, the average velocity of a ganglion and the probability of coalescence given a collision between two ganglia, require additional information. Studies are currently in progress to determine these parameters as functions of the system variables.

Integration of Equations (31) and (32) to obtain the zeroth and first moments will show whether, under a given set of conditions, the oil ganglia tend to organize themselves through coalescence into fewer and larger ones (incipient oil-bank formation) or whether they tend to disintegrate into more numerous and smaller ones, which eventually become stranded again at downstream positions.

The main restriction of the present version of the model is that it applies to immiscible displacement in water wet unconsolidated sandpacks (or similar porous media). Work is underway to expand the model to the case of consolidated porous media, such as sandstones, dolomites, etc.

Prediction of mobilization and of the subsequent motion of oil ganglia through porous media of complex geometry is a problem of major importance in the area of tertiary recovery with chemical flooding. Unfortunately, it is an intransigent problem that has defied numerous efforts by able investigators, even though some of its aspects have been elucidated. The source of the difficulty is manifold.

QUASISTATIC DEFORMATION OF OIL GANGLIA

At the end of secondary flooding, the fraction of the reservoir void space still occupied by oil ganglia is in the range of 0.25 to 0.50.* The objective of tertiary flooding is to recover part of this residual amount of oil. Microscopic studies indicate that residual oil exists in the form of nodular blobs (ganglia) that usually fill one or more (up to fifteen) neighboring pores (Melrose and Brandner, 1974).

Consider, then, a granular porous medium containing oil ganglia at randomly distributed positions, the remaining void space being occupied by formation water. In this work, the walls of the porous medium are assumed to be water wet. According to Melrose and Brandner (1974), the system can be considered water wet if the apparent contact angle, as measured from the water phase, θ is less than 40 deg. Since an oil ganglion occupies a number of adjoining pores, it will occupy not only the space of these pores but will also have numerous protruding appendixes. Each appendix occupies part of a constriction (throat) connecting a pore filled with oil and a pore filled with formation water. The conditions of static equilibrium for such an appendix are

$$P_o - P_w = \gamma_{ow} J_{ow} \tag{1}$$

$$\gamma_{os} = \gamma_{ws} + \gamma_{ow} \cos\theta \tag{2}$$

Equation (1) expresses the condition for hydrostatic equilibrium applicable to each point of the oil-water interface. Equation (2) applies in a similar fashion to every three-phase contact line. Although Equations (1) and (2) are sufficient to express hydrostatic equilibrium, a third relation is necessary to ensure that the oil-water interface is also stable, that is, capable of withstanding small perturbations without collapsing. This was noted by Gibbs, who discussed a particular case in quantitive terms (Miller and Miller, 1956; Melrose 1965, 1968). Melrose (1970) developed the following criterion for configurational stability, based on thermodynamic arguments:

$$\text{For } \theta < 40^\circ \text{ the interface is stable if } \frac{dJ_{ow}}{dV_w} < 0$$

$$\text{For } \theta > 140^\circ \text{ the interface is stable if } \frac{dJ_{ow}}{dV_o} < 0 \tag{3}$$

*In sandpacks and other unconsolidated media, the residual oil is typically in the range 0.1 to 0.2.

Examples of stable and unstable configurations are given in Melrose and Brandner (1974). For a given pore throat geometry and fluid-fluid-solid system there are two limiting configurations of the fluid-fluid interface such that they envelope all stable configurations. The only stable configurations are those for which the magnitude of the curvature J is intermediate to the curvatures of these limiting cases. The maximum curvature is referred to as the drainage curvature J_{dr} and the minimum curvature as the imbibition curvature J_{imb}; the ratio J_{imb}/J_{dr} is equal to ~ 0.65.

At rest the pressure around a ganglion is uniform and so is the pressure inside it. Hence, the pressure difference across the interface of each appendix of a ganglion, $P_o - P_w$, is the same. From Equation (1) it follows that under static conditions the mean curvature of every appendix interface J_{ow} is the same and has a value in the range between J_{imb} and J_{dr}.

If an external pressure gradient ∇P is imposed, the continuous aqueous phase starts flowing with a spatial average velocity given by Darcy's law, $\vec{u} = -(k_e/\mu_w)\,\nabla P$. Mobilization of oil ganglia begins when the flood rate is made sufficiently high for the viscous forces at the oil-water interfaces to start competing successfully with the capillary forces. Not all oil ganglia are mobilized under a given set of conditions. A given ganglion which is not mobilized at a given pressure gradient responds to the normal and shear stresses acting on it by readjusting slightly the lengths of its appendices. Upstream appendices contract so that their curvatures decrease. Downstream appendices elongate, approaching the narrowest cross section of their respective constrictions, so that their curvatures increase. The pressure field within such a ganglion is still uniform, but now the interface curvatures of its appendices are no longer the same, as the external pressure field is not uniform. At each appendix interface, the curvature accords with the local pressure difference between the two phases, if it is assumed that the viscous tangent stresses are relatively small.

OIL GANGLIA IN MOTION

A ganglion which gets mobilized undergoes profound changes. To describe its motion we will adopt the terminology used by Heller (1968) and Melrose and Brandner (1974). The motion of the oil ganglion is episodic, consisting of a series of relatively sudden leaps in the general downstream direction separated by comparatively long periods of slow deformation of the interfaces of the appendixes. Such a sudden leap will be called a ganglion rheon. Each ganglion rheon involves at least two individual displacement events, or rheons (Melrose and Brandner, 1974). One of these will be of the imbibition type, in which water invades a pore which was occupied by the ganglion before the ganglion rheon. This type of rheon is called a hygron. The other will be of the drainage type, in which a pore is invaded by the advancing appendix of the ganglion and gets filled with oil

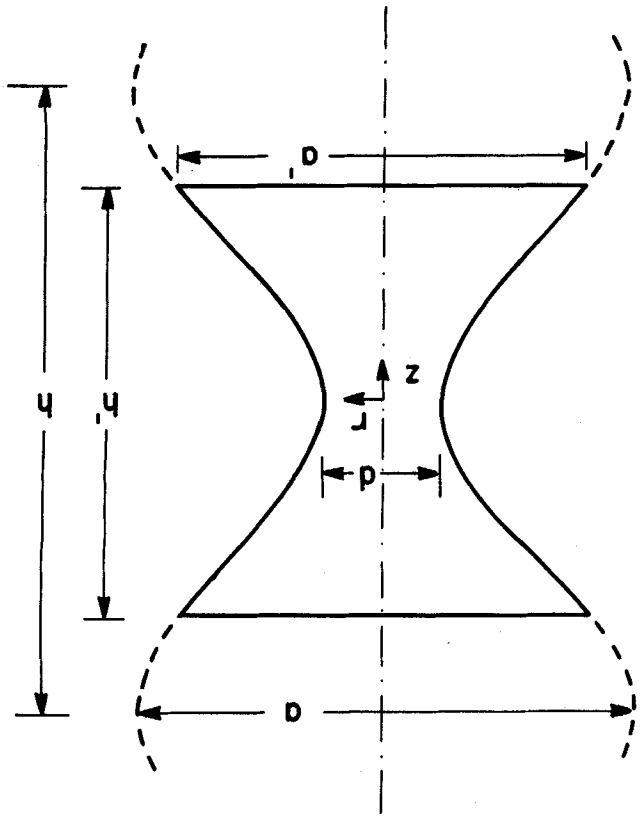

Figure 1. Typical unit cell of the porous medium model ($-h'/2 \leq z \leq h'/2$). The wall profile is a sinusoidal function in z. The segment ($-h/2 \leq z \leq h/2$) is the extended unit cell.

displacing the original mass of water. This type of rheon is called a xeron. The drainage rheon (xeron) usually occurs at the down stream or low pressure side of the ganglion. The imbibition rheon (hygron) usually takes place at the upstream or high pressure side. In porous media with very irregular geometry, it is possible that if the hygron occurs in an unusually large pore, two xerons will be required to accommodate the oil volume. On the other hand, two hygrons may be necessary to supply enough oil to a large xeron. Finally, if the proper conditions for a hygron develop at the middle of a slender oil ganglion, then the resulting ganglion-rheon will involve only the downstream part of the ganglion, while the upstream part remains trapped; this event would result in partition of the ganglion. A given ganglion will continue moving with a succession of ganglion-rheons until either it breaks into two daughter ganglia or it reaches a position where the local pore and constriction topology is such that the ganglion is trapped and cannot be mobilized without appropriate change of the conditions.

Motion of liquid-liquid interfaces is a problem of considerable complexity, even when it takes place in conduits of relatively simple geometry. Tube geometries which are thought to be akin to the configuration of the void space in granular media are those of periodically constricted tubes. The converging-diverging character of the flow channels has been incorporated in the formulation of porous medium models for packings of sand (Payatakes, Tien and Turian, 1973 a,b; Payatakes and Neira, 1977) and its importance for oil displacement has been recognized by Melrose (1970), Slattery (1974), Stegemeier (1976) and Oh and Slattery (1976). Slattery (1974) and Oh and Slattery (1976) have undertaken a theoretical study of the motion of oil blobs in sinusoidal tubes in order to gain some understanding of the episodic motion of ganglia, which in turn can be applied to the complex geometry of oil bearing sandstones.

The problem of liquid-liquid interface motion in conduits of nonuniform cross section becomes further compounded in the presence of surfactants, which are employed in chemical floods to facilitate oil mobilization. The change in the area of the moving interface during a rheon and its possible renewal may lead to a change of the surface concentration of the surfactant and a concomitant change in the interfacial tension. Since such a change would mean that the surfactant concentration at the interface is no longer at equilibrium with the bulk concentration, mass transfer and adsorption-desorption phenomena will be established. That this phenomenon is present and possibly important was demonstrated experimentally by Reisberg and Doscher (1956). Whether or not the mass transfer phenomenon is important in a particular situation where a water-oil interface is moving in an episodic fashion (series of rheons) will depend strongly on the nature and concentration of the surfactant, the flow pattern, the diffusion coefficient, the electrolyte concentration, the rates of adsorption and desorption, the dimensions of the conduit in the neighborhood of the interface and the time scale of the interface motion. A comprehensive, satisfactory solution of this problem still eludes researchers in the area.

DYNAMICS OF OIL GANGLION POPULATIONS

Studies of the fate of solitary oil ganglia provide useful insights and quantitative information but cannot account for the entire spectrum of phenomena taking place during immiscible displacement. This, of course, is due to the fact that they fail to provide for ganglion-ganglion interactions, most notably collision and coalescence.

For given porous medium and immiscible flood conditions, only a number fraction of the entrapped oil ganglia gets mobilized. As discussed earlier, mobilized ganglia have a strong tendency to break into smaller ones. The ensuing smaller daughter ganglia become gradually stranded anew through random encounters with narrow throats. This tendency for deterioration through breakup and stranding can lead to very small microdisplacement efficiencies; fortunately, the situation is ameliorated by coalescence between colliding pairs of ganglia and remobilization.

In order to describe mathematically the collective fate of oil ganglion populations, we propose the following strategy:

1. Formulate a suitable porous medium model.
2. Develop a method to calculate proabilities for the mobilization, breakup and stranding of solitary oil ganglia.
3. Determine an expression for the average velocities of oil ganglia of different sizes.
4. Determine axial and lateral ganglion dispersion coefficients.
5. Determine the probability of coalescence given a collision between two ganglia.
6. Develop ganglia population balances.
7. Integrate the ganglion population balances (the zeroth and first moments may suffice.).

Obviously, formulation of a realistic porous medium model will be the cornerstone for the entire scheme, as the porous structure is central to and permeates every facet of the mobilization and subsequent fate of oil ganglia. Other parameters of primary importance, as they emerge from this analysis, are the capillary number, the average velocity of oil ganglia, the rate of collision and the probability of coalescence given a collision.

SPECIFICATIONS FOR THE POROUS MEDIUM MODEL

The objective of a porous medium model is to provide a reasonable idealization of the geometrical structure of a particular class of porous media, based on which a transport process of interest can be treated mathematically. To this end, the model should incorporate the most relevant characteristics of the prototype, while its complexity should be held at a manageable level. From these considerations, it becomes clear that the porous medium model which is most appropriate for a given modeling application depends not only on the porous medium but also on the process under study.

In order to formulate a realistic model suitable to serve as basis for the modeling of oil ganglion motion, breakup and

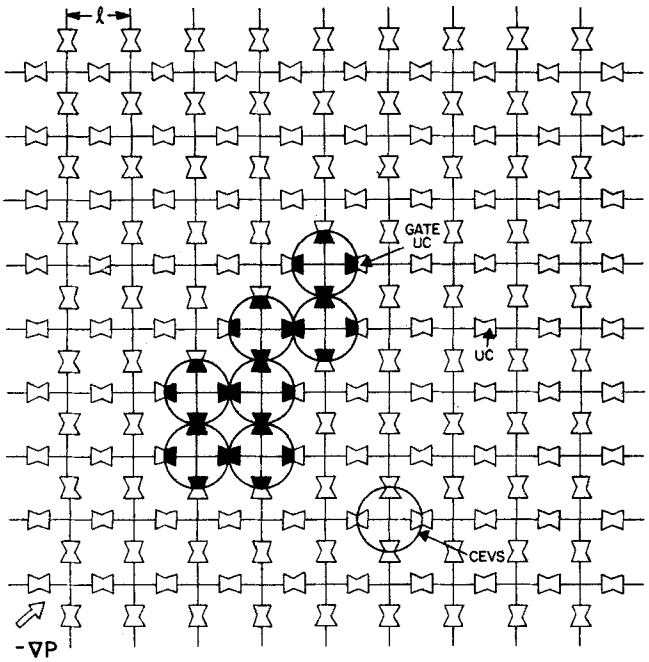

Figure 2. Two-dimensional depiction of idealized cubic network of unit cells. A conceptual elemental void space (CEVS) and a unit cell (UC) are identified. An idealized oil ganglion occupying seven adjoining pores is also shown.

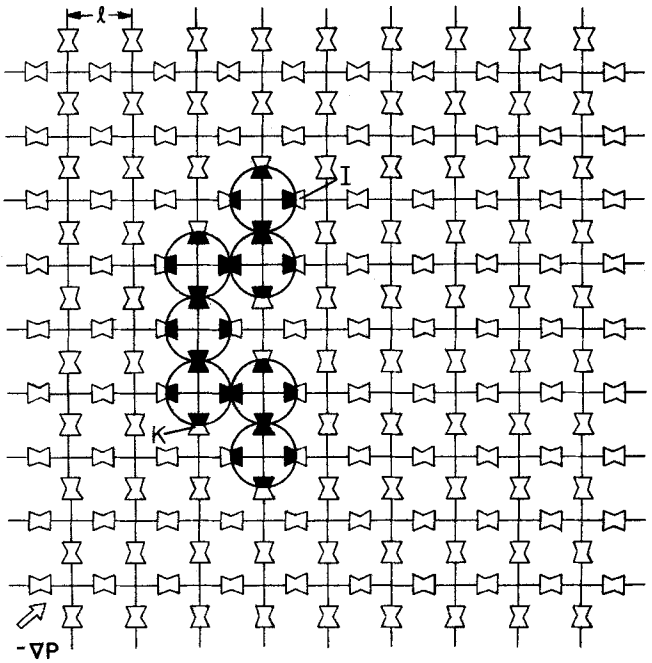

Figure 3a. Two-dimensional depiction of oil ganglion fission. (a). Mother ganglion before the ganglion-rheon. The pair of unit cells through which the xeron (I) and hygron (K) take place are indicated.

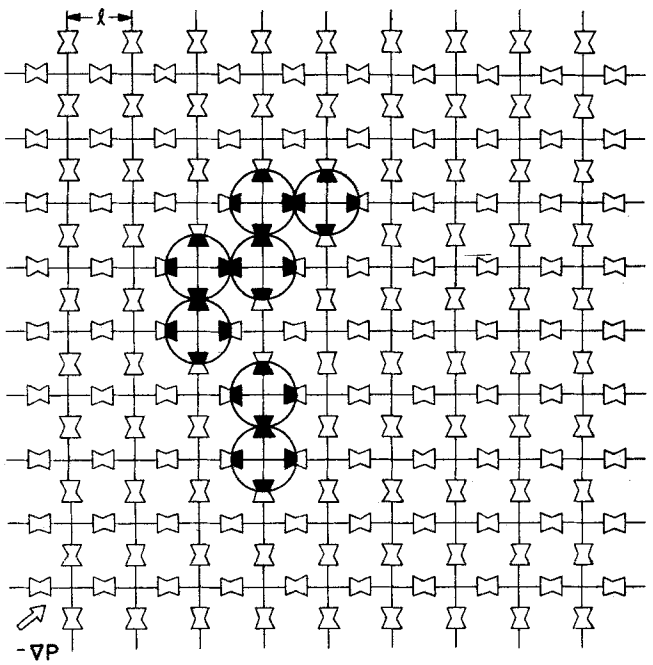

Figure 3b. Two dimensional depiction of oil ganglion fission. (b). Daughter ganglia resulting from the mother ganglion of Figure 3 (a).

coalescence, the following important characteristics must be incorporated in the design:

1. The converging-diverging character of the flow channels must be retained.
2. The effective size distribution of the constrictions connecting adjacent cavities should be in close agreement with that of the actual porous medium.
3. The model should have the same porosity as that of the prototype.
4. The model should have the same number of constrictions per unit volume as the prototype.
5. The degree of pore interconnectivity should reflect that of the prototype.
6. The model should have the same number of pores (not to be confused with constrictions) as the prototype.
7. The model permeability and relative permeability should agree well with those of the prototype.
8. The model should be such that an oil ganglion could be identified within its framework with regard to size, shape and position coordinates.
9. The local topology of the model should afford conditions leading to ganglion-rheons in the prototype.
10. The model should be of manageable complexity, lending itself at least to simulation studies of ganglion motion, fission and coalescence, and preferably to analytical treatment as well.

A model which is believed to meet rather satisfactorily these specifications is described in the following section.

FORMULATION OF THE POROUS MEDIUM MODEL

The model proposed here is a network of interconnected unit cells of the constricted tube type. A unit cell has axial symmetry, and its wall profile is a sinusoidal function. Figure 1. Let $r_w(z)$ be the distance of the wall from the axis at axial position z. It is

$$r_w(z) = \tfrac{1}{4}[(a+d) - (a-d)\cos(\frac{2\pi z}{h})] \qquad (4)$$

The unit cell is the segment corresponding to $-h'/2 \leqq z \leqq h'/2$, Figure 1. The reason for this formulation is that it maintains the realistic dimensions of the unit cells of the P-T-T (Payatakes, Tien and Turian, 1973) porous medium model, and at the same time it makes it possible for the model to retain the porosity of the prototype as well as the number of constrictions per unit volume. In analogy with the P-T-T porous medium model, we set*

$$a = c_1 d\ ,\ h = c_2 d \qquad (5)$$

$$a' = \tfrac{1}{2}[(c_1+1)-(c_1-1)\cos(\pi c_3)]d\ ,\ h' = c_2 c_3 d \qquad (6)$$

As in the case of the P-T-T model, we have

$$c_1 = \left[\frac{\epsilon(1-S_{wi})}{(1-\epsilon)}\frac{\langle d_g^3\rangle}{\langle d_c^3\rangle}\right]^{1/3},\ c_2 = \frac{\langle d_g\rangle}{\langle d_c\rangle} \qquad (7)$$

The constriction size distribution is obtained from the initial

*The assumptions expressed by Eq. (5) are not justified in the case of consolidated porous media. In the latter case they will be relaxed; a and h will be assumed to be independent random variables and will be calculated from the size distributions of the principal axes of the chambers.

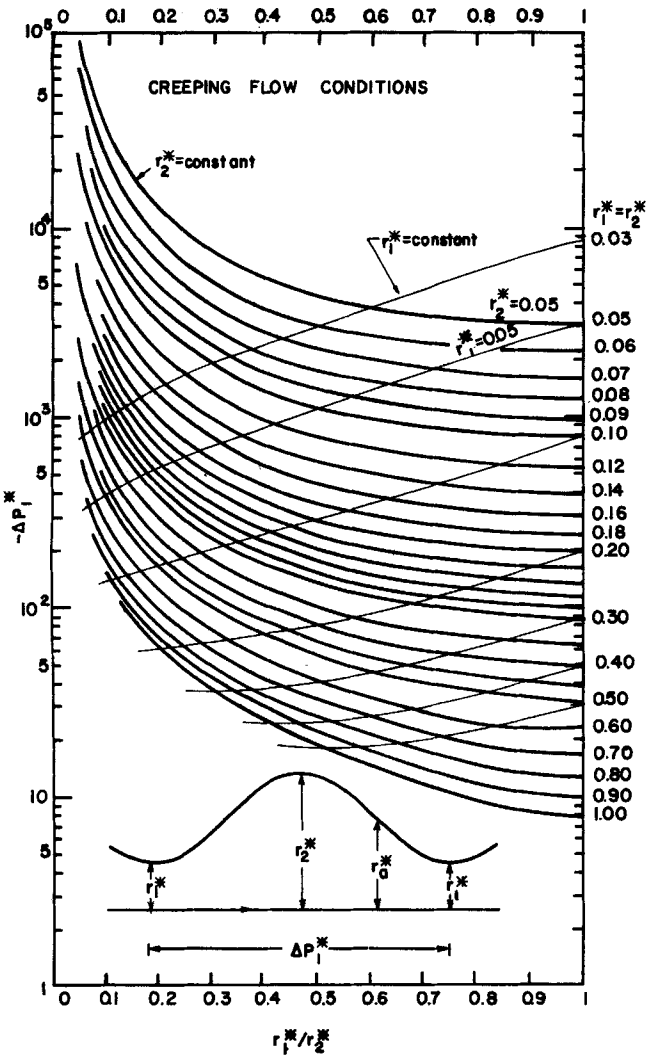

Figure 4. Plot of values of $-\Delta P_1^*$ vs. r_1^*/r_2^* with r_2^* as the parameter. A number of lines with constant r_1^* are also shown. (From Neira and Payatakes, 1979.)

drainage curve (Payatakes et al., 1973; Payatakes and Neira, 1977). The constant c_3 is determined below.

Consider a pore (cavity) of the porous medium and the narrow throats connecting it with its adjacent pores. Consider the narrowest cross section of each one of these satellite throats. The void space composed of the pore and its satellite throats up to the respective narrowest cross sections will be denoted as an elemental void space. An elemental void space in a packing of grains has a number of satellite throats, n_{th}, which varies in the range 4 to 6, with average value around 5. For simplicity, we will assume that the unit cell network is a regular one. The tetrahedric network corresponds to $n_{th} = 4$, whereas the cubic network corresponds to $n_{th} = 6$. Melrose's (1965) analysis of imbibition and drainage indicates that the cubic network is a reasonable assumption for a random pack of uniform spheres or grains.

A void volume balance gives

$$\epsilon(1-S_{wi}) = N_{uc}\langle V_{uc}\rangle = \tfrac{1}{2}\, n_{th} N_p \langle V_{uc}\rangle = \tfrac{1}{2}\, n_{th}\ell^{-3}\langle V_{uc}\rangle \quad (8)$$

We have

$$\ell = \left[\frac{\pi}{6(1-\epsilon)}\langle d_g^3\rangle\right]^{1/3};\ N_p = \ell^{-3};\ N_{uc} = \tfrac{1}{2}\, n_{th}\ell^{-3} \quad (9)$$

Using Equations (4) and (5), one obtains by integration

$$V_{uc} = \frac{d^3}{16}[c_2(c_1+1)^2\pi c_3 - 2c_2(c_1^2-1)\sin\pi c_3 + \tfrac{1}{2}\, c_2(c_1-1)^2(\pi c_3+\sin\pi c_3\cos\pi c_3)] \quad (10)$$

Equations (7) to (10) together give

$$c_2(c_1+1)^2\pi c_3 - 2c_2(c_1^2-1)\sin\pi c_3 + \tfrac{1}{2}\, c_2(c_1-1)^2(\pi c_3+\sin\pi c_3\cos\pi c_3) = \frac{16\pi c_1^3}{3n_{th}} \quad (11)$$

which can be solved readily to obtain c_3[c_1 and c_2 are given by Equations (7)].

Equations (6), (7) and (11) together with the experimentally determined constriction size distribution and grain size distribution define completely the distributions of the characteristic lengths (a', d, h') or (a, d, h) of the UC's.

To account for the interconnectivity between pores, it will be assumed that the unit cells are interconnected, forming a cubic network in the case of $n_{th} = 6$ and a tetrahedric network in the case of $n_{th} = 4$.

Cubic Lattice

A two-dimensional representation of the cubic network is given in Figure 2. This network can be considered as a cubic matrix of conceptual nodes (with no volume or resistance to flow), interconnected with randomly sized unit cells. The step of the network equals the length of periodicity given by Equation (9). Each node is connected to six unit cells (the pair normal to the plane of paper is not shown). The unit cells have the shape shown in Figure 1 with random size, even though for the sake of simplicity they are depicted in Figure 2 with a simple uniform symbol, irrespective of their size. One node and the adjacent six half-unit cells comprise a conceptual elemental void space (CEVS).

If a given elemental void space is occupied by oil, the corresponding CEVS is assumed to be occupied by oil, too. According to the model, when a CEVS is occupied by oil, the oil fills the six half-unit cells that belong to the CEVS under consideration. The representation of an oil ganglion occupying several adjacent pores is made in a similar way by filling the half-unit cells of the appropriate CEVS's Figure 2. Unit cells containing an oil-water interface are called gate unit cells (GUC). This is a realistic and convenient method of describing the size, shape and position coordinates of an oil ganglion. Furthermore, since the unit cells filled with oil are highly interconnected and the gate unit cells are randomly sized, the basis for mathematical simulation is present.

Tetrahedric Lattice

The shortest distance between two nodes of a tetrahedric network δ is given by

$$\delta = \frac{\sqrt{3}}{2}\ell \approx 0.866\ell \quad (12)$$

The side of each elemental tetrahedron κ is given by

$$\kappa = 2\sqrt{\frac{2}{3}}\,\delta = \sqrt{2}\ell \cong 1.414\ell \quad (13)$$

Conceptual elemental void spaces and oil ganglia are defined as in the case of the cubic lattice. The main differences are that there are 4 half-unit cells in each CEVS and that the angles between intersecting unit cell axes are $2\sin^{-1}\sqrt{2/3} \approx 0.608\pi$ rather than $\pi/2$. It should also be noted that whereas c_1 and c_2 are the same for cubic and tetrahedric lattices, c_3 is slightly larger in the case of the tetrahedric lattice [Equation (11)].

QUASISTATIC CRITERION FOR THE MOBILIZATION AND BREAKUP OF OIL GANGLIA

In studying the motion and fission of oil ganglia, their shape, size, orientation relative to the macroscopic pressure gradient and topology of occupied space are important factors. Generalizing and extending the Melrose-Brandner (1974) criterion, Ng and Payatakes (1980) developed an algorithm for the determination of the conditions for mobilization, locations of the xeron and hygron and the conditions for fissions, Figure 3. This algorithm

TABLE 1. EXPERIMENTAL AND THEORETICAL ANALYSIS OF TYPICAL RANDOM PACKING OF GLASS SPHERES

Experimental		Theoretical	
Exper.quant.		Exper.quant.	
ϵ	0.40	Unit cell geometry:	
Microscopic analysis:		c_1	2.141
$\langle d_g \rangle$, mm	0.470	c_2	2.652
$\langle d_g^3 \rangle$, mm^3	1.038×10^{-1}	c_3 (cubic)	0.531
Initial drainage curve:		c_3 (tetrahedric)	0.666
S_{wi}	0.11	ℓ, mm	0.449
$\langle d_c \rangle$, mm	0.177	r_1^*	0.1885
$\langle d_c^3 \rangle$, mm^3	6.272×10^{-3}	r_2^*	0.4035
$\langle d_c^4 \rangle$, mm^4	1.258×10^{-3}	Collocation solution:	
		$-\Delta P_1^*$ (r_1^*, r_2^*)	86.7
Experimental permeability			
k, mm^2	2.34×10^{-4}	Calculated permeability:	
		k, mm^2 (cubic)	3.97×10^{-4}
		k, mm^2 (tetrahedric)	2.30×10^{-4}

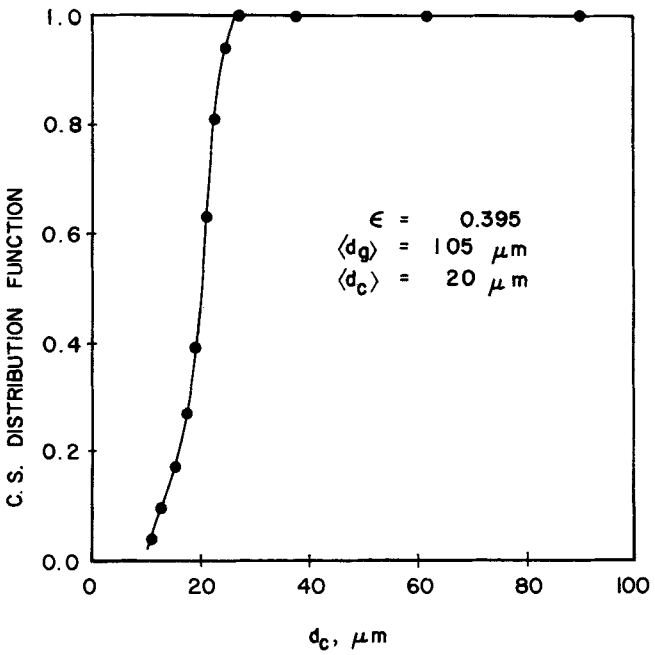

Figure 5. Constriction size distribution of 100×200 sandpack.

will not be reiterated here, but the main conclusions derived from Monte Carlo simulations, based on its repeated use, are given later in this work.

Coalescence of Oil Ganglia

If a ganglion while moving contacts another ganglion (moving or stranded), the two may coalesce. A finite time period is required for the drainage of the aqueous film separating the two ganglia. When this film becomes thin enough, instability develops and the film collapses, resulting in the coalescence of the two ganglia. However, it is possible that before the separating film collapses, a new rheon may separate again the two ganglia [Ng, Davis and Scriven, 1978], in which case coalescence is averted.

SINGLE-PHASE FLOW THROUGH A UNIT CELL

The flow through an extended unit cell, Figure 1, is assumed to be identical to that through a segment of the corresponding infinitely long periodically constricted tube. The pressure drop along the extended unit cell ($-h/2 \leqq z \leqq h/2$) is assumed to be given by

$$-\Delta P_h = h|\nabla P| \cos\alpha = c_2 d|\nabla P| \cos\alpha \tag{14}$$

The pressure gradient is oriented at an arbitrary angle relative to the unit cell network, which is isotropic. This flow problem was solved with a collocation method in Neira and Payatakes (1979).

A dimensionless pressure drop is defined by

$$\Delta P_h^* = \frac{\Delta P_h}{\rho v_o^2} \tag{15}$$

Under creeping flow conditions, we have

$$\Delta P_h^* = \frac{\Delta P_1^*(r_1^*, r_2^*)}{N_{Re}} \; ; \; N_{Re} = \frac{h v_o}{\nu} \tag{16}$$

ΔP_1^* can be calculated by integration of the viscous dissipation function. Neira and Payatakes (1979) performed this calculation for a large number of values of (r_1^*, r_2^*) and presented the results in graph form, Figure 4.

ABSOLUTE PERMEABILITY

Cubic Lattice

Assuming a cubic lattice, one can easily show from continuity considerations

TABLE 2. EXPERIMENTAL AND THEORETICAL ANALYSIS OF TYPICAL RANDOM PACKING OF 100×200 SAND

Experimental		Theoretical	
Exper.quant.		Exper.quant.	
ϵ	0.395	Unit cell geometry:	
Microscopic analysis:		c_1	4.16
$\langle d_g \rangle$, mm	0.105	c_2	5.25
$\langle d_g^3 \rangle$, mm^3	1.16×10^{-3}	c_3 (cubic)	0.684
Initial drainage curve:		c_3(tetrahedric)	0.798
S_{wi}	0.09	l, mm	0.100
$\langle d_c \rangle$, mm	0.020	r_1^*	0.095
$\langle d_c^3 \rangle$, mm^3	9.54×10^{-6}	r_2^*	0.396
$\langle d_c^4 \rangle$, mm^4	0.22×10^{-6}	Collocation solution:	
		$-\Delta P_1^*$ (r_1^*, r_2^*)	194.26
Experimental permeability			
k, mm^2	3.55×10^{-6}	Calculated permeability:	
		k, mm^2 (cubic)	2.46×10^{-6}
		k, mm^2 (tetrahedric)	1.42×10^{-6}

$$k = k_w = k_o = \frac{\pi c_2^2 \langle d_c^4 \rangle}{4\ell^2(-\Delta P_1^*)} \tag{17}$$

The flow rate through a unit cell q_{uc} and the superficial velocity $\vec{u}$ through the porous medium are given by

$$q_{uc} = \frac{\pi c_2^2 d^4}{4\mu(-\Delta P_1^*)} |\Delta P| \cos\alpha \lessgtr \vec{u} = -\frac{\pi c_2^2 \langle d_c^4 \rangle}{4\mu\ell^2(-\Delta P_1^*)} \nabla P \tag{18}$$

Tetrahedric Lattice

In this case, we have

$$k = k_w = k_o = \frac{\sqrt{3}\,\pi c_2^2 \langle d_c^4 \rangle}{12\ell^2(-\Delta P_1^*)} \tag{19}$$

$$q_{uc} = \frac{\pi c_2^2 d^4}{4\mu(-\Delta P_1^*)} |\nabla P| \cos\alpha\,;\ \vec{u} = -\frac{\sqrt{3}\,\pi c_2^2 \langle d_c^4 \rangle}{12\mu\ell^2(-\Delta P_1^*)} \nabla P \tag{20}$$

Sample Calculations of Absolute Permeability

The permeability of a random packing of nearly uniform glass beads with average diameter of 470 μm and having porosity $\epsilon = 0.40$ is calculated with the present model and compared with the experimental value reported by Payatakes et al. (1973a). The constriction size distribution of this packing is also reported in Payatakes et al. (1973a); the analysis of the porous medium is summarized in Table 1.

As should be expected, the experimental permeability value 2.34×10^{-4} mm^2 is smaller than that calculated by assuming a cubic network, 3.97×10^{-4} mm^2, and it is slightly larger than the one based on the assumption of a tetrahedric network, namely, 2.30×10^{-4} mm^2. The last value differs from the experimental one by only -1.7%.

Agreement with the experimental permeability of packings of fine, relatively multisized sand grains is not as good as the one observed above. Consider, for instance, the 100×200 sandpack studied by Leverett (1941). The constriction size distribution for this sandpack, Figure 5, was obtained with the method developed in Payatakes et al. (1973) using the initial drainage data reported by Leverett. Other pertinent parameters for this porous medium are summarized in Table 2. The theoretical permeability based on the cubic network is $k = 2.46 \times 10^{-6}$ mm^2, a value which is 31% lower than the experimental value 3.55×10^{-6} mm^2, reported by Leverett. This discrepancy is to be expected in view of the fact that the 100×200 sandpack deviates appreciably from a random packing of nearly uniform grains. Furthermore, some channeling through packings of very fine particles is quite likely (caused by the existence of regions of loose packing), and this would tend to increase the experimental permeability. It should be added that the above analysis does not involve any adjustable parameters (such as tortuosity), but it is based on first principles and independent experimental measurements, as well as on a number of reasonable assumptions.

RELATIVE PERMEABILITY TO WATER

Consider a packed bed, the void space of which is filled with oil and water. Let ϕ_w and ϕ_o be the number fractions of unit cells which are occupied completely by water and oil, respectively. Also, let ϕ_{ow} be the fraction of the population of unit cells that contains an oil-water interface. Obviously

$$\phi_w + \phi_{ow} + \phi_o = 1 \tag{21}$$

Before we can proceed, we need to establish one more relationship between ϕ_w, ϕ_o and ϕ_{ow}. At large water saturations, the oil exists in the form of relatively elongated oil ganglia. It is reasonable to assume that as $\phi_w \to 1$, $(S_w \to 1)$ the ratio ϕ_{ow}/ϕ_o tends to some constant value η of the order of $\eta \approx \frac{1}{2} n_{th}$, and it does so with nearly zero gradient. On the other hand, for large

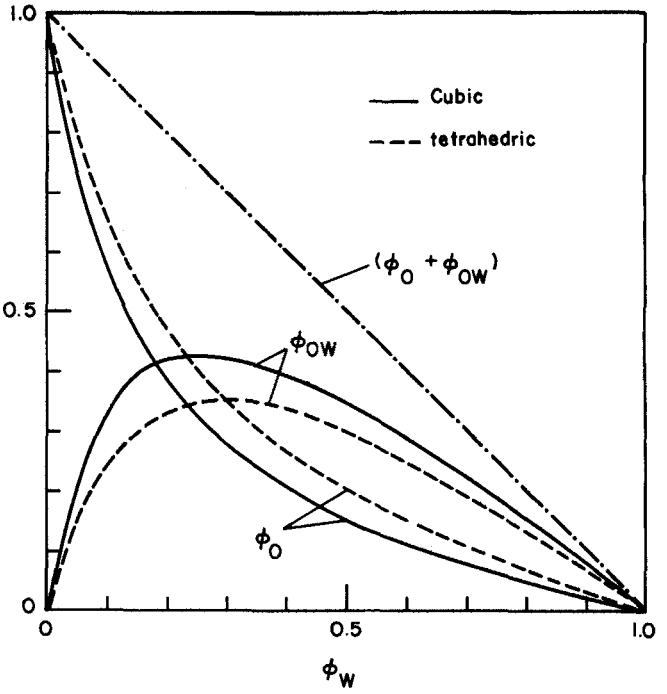

Figure 6. Estimated dependence of ϕ_o and ϕ_{ow} on ϕ_w, assuming $\eta = \frac{1}{2} n_{th}$.

oil saturation values, that is, as $\phi_w \to 0$, $(S_w \to S_{wi})$, the ratio ϕ_{ow}/ϕ_o vanishes. Assuming a binomial approximation (this is better than the linear approximation used in Payatakes, Flumerfelt and Ng, 1978), we get

$$\frac{\phi_{ow}}{\phi_o} \cong \eta\,\phi_w(2 - \phi_w) \tag{22}$$

Equations (21) and (22) give

$$\phi_o \cong \frac{(1 - \phi_w)}{[1 + \eta\phi_w(2-\phi_w)]}\ ;\ \phi_{ow} \cong \frac{\eta\phi_w(2-\phi_w)(1-\phi_w)}{[1 + \eta\phi_w(2-\phi_w)]} \tag{23}$$

These functions are plotted in Figure 6.

Making now a water volume balance, we get

$$\epsilon S_w = \epsilon S_{wi} + N_{uc}[\phi_w \langle V_{uc} \rangle_w + \tfrac{1}{2}\phi_{ow} \langle V_{uc} \rangle_{ow}] \tag{24}$$

Here $\langle V_{uc} \rangle_w$ stands for the average volume of unit cells filled only with water and $\langle V_{uc} \rangle_{ow}$ for the average volume of unit cells containing an oil-water interface. We have also assumed that unit cells containing an interface are filled half and half with water and oil.

From Equations (10) and (11) we have

$$V_{uc} = \frac{\pi c_1^3}{3n_{th}} d^3\ ;\ \langle V_{uc} \rangle = \frac{\pi c_1^3}{3n_{th}} \langle d_c^3 \rangle \tag{25}$$

Using Equations (7), (9), (23) and (25), Equation (24) becomes

$$S_w = S_{wi} + (1 - S_{wi})\phi_w \left\{ \frac{\langle d_c^3 \rangle_w}{\langle d_c^3 \rangle} + \frac{\eta(2-\phi_w)(1-\phi_w)}{2[1+\eta\phi_w(2-\phi_w)]} \frac{\langle d_c^3 \rangle_{ow}}{\langle d_c^3 \rangle} \right\} \tag{26}$$

Assuming that water flow takes place only in unit cells that are filled completely with water, the effective permeability is obtained readily as

$$\left.\begin{aligned} k_e &= \frac{\pi c_2{}^2}{4\ell^2(-\Delta P_1^*)} \phi_w \langle d_c{}^4 \rangle_w \quad \text{(cubic lattice)} \\ k_e &= \frac{\sqrt{3}\,\pi c_2{}^2}{12\ell^2(-\Delta P_1^*)} \phi_w \langle d_c{}^4 \rangle_w \quad \text{(tetrahedric lattice} \end{aligned}\right\} \tag{27}$$

Hence, the relative permeability to water k_{rw} is given by

$$k_{rw} = \frac{k_e}{k_w} = \frac{\langle d_c{}^4 \rangle_w}{\langle d_c{}^4 \rangle} \phi_w \tag{28}$$

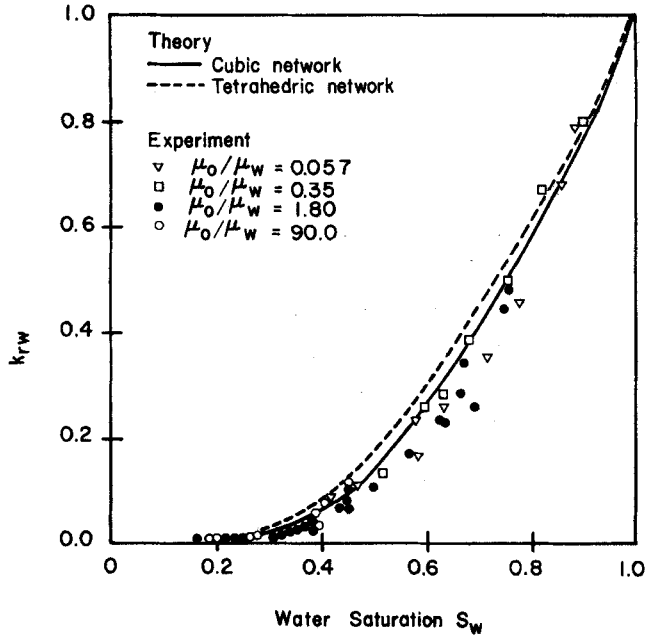

Figure 7. Experimental and theoretical relative permeability to water vs. water saturation for a pack of 100×200 sand. Experimental data after Leverett (1939).

Equations (26) and (28) give the sought relationship between k_{rw} and S_w in parametric form with ϕ_w as the parameter, provided that $<d_c^3>_w$, $<d_c^4>_w$ and $<d_c^3>_{ow}$ are available. These last quantities can be obtained routinely if we know the constriction size distribution of the unit cells filled with water and that of the unit cells that contain an oil-water interface.

Experimental determination of k_{rw} is ordinarily made with slow invasion of water into the porous matrix. Under these conditions, the displacement is taking place mainly owing to imbibition; in this case, oil is withdrawn first through the smaller channels and water is imbibed to fill the spaces being evacuated. In such experiments, then, the population of unit cells filled with water will correspond to the range of low constriction diameter values.*

Let f_{d_c} be the constriction diameter frequency function (Payatakes and Neira, 1977). Let d_w be defined by

$$\phi_w = \int_{d_{c,\min}}^{d_w} f_{d_c}(x)dx \tag{29}$$

that is, d_w is such that unit cells with $d<d_w$ are filled only with water and unit cells with $d>d_w$ are not. Clearly, d_w is a function of ϕ_w and can be determined readily if f_{d_c} is available. Then

$$<d_c^m>_w = \frac{1}{\phi_w}\int_{d_{c,\min}}^{d_w(\phi_w)} x^m f_{d_c}(x)dx \;;$$

$$<d_c^m>_{ow} = \frac{1}{(1-\phi_w)}\int_{d_w(\phi_w)}^{d_{c,max}} x^m f_{d_c}(x)dx \tag{30}$$

Sample Calculations of Relative Permeability to Water

The relative permeability to water for 100×200 sand was determined by Leverett (1939) under imbibition conditions, using an oil-water mixture. The experimental constriction size distribution curve for such a packing, Figure 5, was estimated with the method developed in Payatakes et al. (1973a) using the initial drainage data reported by Leverett (1941). Leverett's experimental data and the corresponding theoretical curves are given in Figure 7 for $\eta \approx \frac{1}{2}n_{th} = 2$ (tetrahedric network) and for $\eta \approx n_{th} = 3$ (cubic network). The agreement between the experimental data and the present theoretical results is excellent. Note that the k_{rw} vs. S_w data are virtually independent of the ratio of the viscosities μ_o/μ_w, under imbibition conditions. This also is in agreement with the theoretical results.

*If, on the other hand, the water is forced into the porous structure rapidly (under positive pressure), there is a strong tendency for water to invade through large pores (Moore and Slobod, 1956), and a larger relative permeability value is obtained.

SIMULATION OF THE FATE OF SOLITARY OIL GANGLIA

This study provides information pertaining to the behavior of individual ganglia and forms the basis for the analysis of the collective behavior of large populations of interacting oil ganglia. The latter problem, in turn, is central to the understanding of oil-bank formation and/or attrition.

In order to demonstrate the usefulness of the present model in simulating the fate of solitary oil ganglia, sample calculations pertaining to a 100×200 sandpack were performed. The constriction size distribution for this porous medium is given in Figure 5; other pertinent parameters were given in Table 2.

The details of the computer aided stochastic simulation and a comprehensive summary of the results are given in Ng and Payatakes (1980). Here we simply present an outline for the sake of completeness.

For simplicity, the simulations were made with a two-dimensional version of the cubic lattice, as shown in Figure 2. For oil ganglia composed of a given number of CEVS's, say seven, the simulation begins by generating a randomly shaped conceptual ganglion (Figure 2) and by assigning random values to the diameters of the gate unit cells, according to the distribution in Figure 5. After each rheon, random dimensions are assigned to the newly occupied gate unit cells. The error introduced by omitting the third dimension is expected to be significant only for relatively large ganglia, say ganglia occupying ten or more elemental void spaces. The results were obtained for zero contact angle, $\theta=0$, and can be classified in two groups: individual stochastic realizations and expected behavior (expressed in terms of probabilities).

Individual Stochastic Realizations

A typical realization of the fate of a seven CEVS ganglion for $N_{Ca} = \mu_w V_f/\gamma_{ow} = 1.07\times10^{-3}$ is shown in Figure 8. As can be seen, the ganglion undergoes a series of three rheons, changing position and shape with each rheon, and then it breaks into two daughter ganglia. It so happens in this particular example that the smaller of the daughter ganglia becomes stranded immediately upon birth, while the larger one goes on (for a short while, anyway).

This breakup phenomenon followed by eventual stranding of the daughter ganglia is observed for ganglia of all sizes larger than one CEVS. Of course, if the value of the capillary number is high enough to mobilize a one CEVS ganglion even through the narrowest of constrictions, breakup is not followed by eventual stranding. However, such high capillary number values ($N_{Ca} > 10^{-2}$) cannot be easily achieved and maintained in a reservoir.

Expected Behavior of Solitary Ganglia

Various aspects of the expected behavior of mobilized ganglia can be obtained by averaging the results of a large number of realizations (runs). In each run the initial shape of the ganglion is generated by filling a given number of adjoining CEVS's at random. The rationale behind this policy is that even though every ganglion during its short lifetime strives to acquire a preferred elongated configuration (Ng and Payatakes, 1980), at birth (through breakup of a larger ganglion or coalescence of two smaller ones) its shape will be more nearly arbitrary. The total length of computation time required for one realization is of the order of 1s or less, even for ten CEVS ganglia. Several hundred runs are made for each ganglion size, and the results are averaged.

A convenient and useful way to summarize the results of the stochastic simulation is to report the probability of mobilization

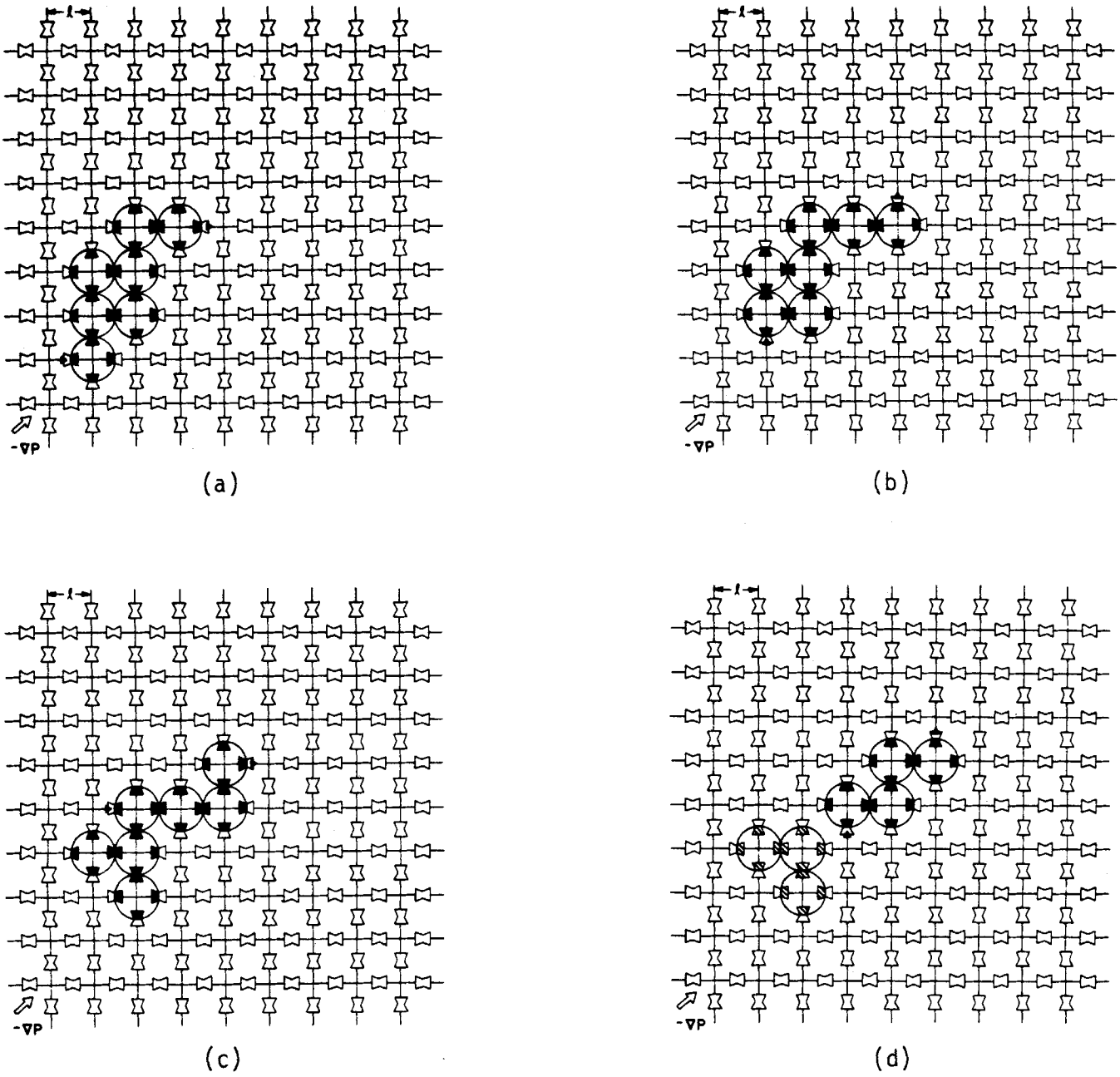

Figure 8. Typical stochastic realization of the fate of a seven CEVS ganglion introduced randomly into a 100×200 sandpack; $N_{Ca} = 1.07\times10^{-3}$. (a). Initial position and shape. (b). Ganglion after one rheon. (c). Ganglion after two rheons. (d). The ganglion breaks in two daughter ganglia during the third rheon. The three CEVS daughter ganglion remains stranded, while the four CEVS ganglion undergoes at least one more rheon.

(at least one rheon from the initial position) M, the probability of breakup per rheon B and the probability of stranding per rheon S as functions of the capillary number N_{Ca} and the size of the ganglion. Clearly, M+B+S = 1. Such results for seven CEVS ganglia are plotted in Figure 9. Similar results for ganglion sizes from 1 to 50 CEVS's are given in Ng and Payatakes (1980) for the case of the 100×200 sandpack. The major conclusions from these simulations are:

1. Oil ganglia tend to be elongated while moving.
2. The probability of stranding per rheon decreases rapidly with N_{Ca} and ganglion size; it is negligible for large ganglia (>ten CEVS) when $N_{Ca}>5\times10^{-3}$ (in complete agreement with previous experience).
3. The probability of breakup per rheon for ganglia larger than two CEVS is quite large, typically 0.10 to 0.17.*
4. The probability that medium sized and large (>three CEVS) solitary ganglia will not break into daughter ganglia during a series of, say, thirty rheons is virtually nil.
5. The probability of stranding of small (one to five CEVS) ganglia per rheon is significant, even in a 100×200 sandpack. Only for $N_{Ca}>10^{-2}$ is this danger completely averted.
6. For N_{Ca} values significantly below the critical one ($\sim10^{-2}$), the probability that a small (one to five CEVS) ganglion will not get stranded during a series of, say, fifty rheons is virtually nil. It is useful to recall that in the present case the distance traveled with fifty rheons is substantially less than 50ℓ = 5 mm.

These conclusions indicate clearly the crucial role played by coalescence and set the stage for the considerations of the following section.

POPULATION BALANCE APPROACH TO OIL GANGLION DYNAMICS

The seemingly pessimistic results from the simulation of the

*This may be somewhat inflated for large ganglia owing to the omission of the effect of three dimensionality.

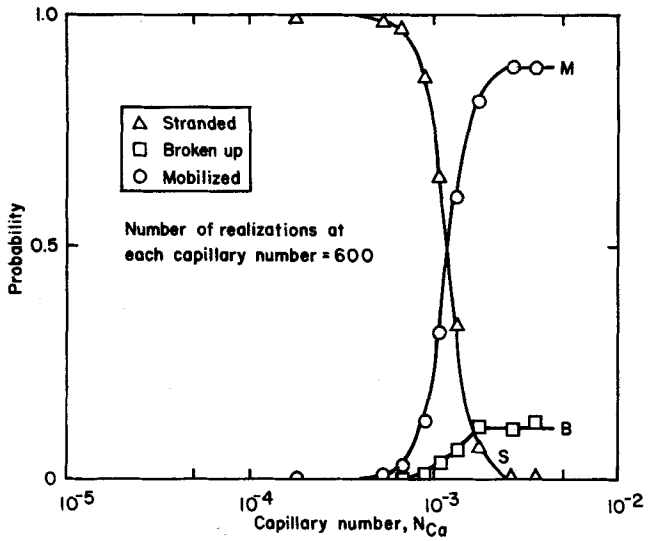

Figure 9. Plot of the probabilities M, B and S vs. capillary number for seven CEVS ganglia in a 100×200 sandpack. Contact angle $\theta = 0$.

fate of solitary oil ganglia indicate clearly that the interaction of neighboring ganglia is of paramount importance in averting monotonic deterioration of the initial population of ganglia.

A method is developed here (see also Payatakes, Flumerfelt and Ng, 1978a, b) which utilizes the results pertaining to solitary ganglia and which at the same time accounts for interactive effects between ganglia.

Initially, oil ganglia of various volumes and shapes are distributed randomly throughout the reservoir. As the chemical flood commences, the leading slug of concentrated surfactant solution starts mobilizing the oil ganglia it engulfs. As a worst case analysis, we assume immiscible displacement. For given porous medium and flood conditions, only a fraction of the subpopulation of oil ganglia with volume in a given range $[v, (v+\Delta v)]$ gets mobilized. Mobilized ganglia of given volume are assumed to move into the direction of the flood with a corresponding mean velocity and also to undergo dispersion in the axial and lateral directions. Larger oil ganglia are easier to mobilize, and therefore should be expected to migrate at higher average velocities (undergoing more rheons per unit time).* Collisions between oil ganglia take place because of this difference in mean axial velocities (interception) and also because of the axial and lateral dispersion. If two ganglia collide and remain in close contact sufficiently long, they will coalesce into a new larger ganglion. This beneficial growth process is curbed to a certain extent by the continual fissioning of large ganglia into smaller ones. If the daughter ganglia from a fission are sufficiently small, they have a high risk of getting stranded by encountering a set of narrow throats. In the final analysis, the competition between coalescence on one hand and fission and/or stranding on the other will determine whether an oil bank is formed or not. In the latter case, the oil ganglia fail to organize into larger (and fewer) ones; instead, they remain numerous and small, keep losing ground with respect to the flood front and eventually become stranded.

Mathematical Formulation

Consider a layer of the oil reservoir with differential thickness Δz, where z is the Cartesian coordinate in the direction of the flood, Fig. 10. This differential control volume and its surrounding contain multisized oil ganglia, either moving or stranded. Let a ganglion with volume in the range v to $v + \Delta v$ be denoted as a v ganglion. Making number balances for moving and stranded v ganglia, we get two coupled integrodifferential equations of the birth-death type (for a detailed derivation see Payatakes, Flumerfelt and Ng, 1978a):

$$\frac{\partial n(z,t;v)}{\partial t} + \bar{u}_z(v;\underline{a}_1)\frac{\partial n(z,t;v)}{\partial z} - D_z(v;\underline{a}_1)\frac{\partial^2 n(z,t;v)}{\partial z^2}$$
$$= -n(z,t;v)\{\bar{u}_z(v;\underline{a}_1)[\lambda(v;\underline{a}_2) + \phi(v;\underline{a}_2)]$$
$$+ \int_0^\infty K_{11}(u,v;\underline{a}_4)n(z,t;u)du$$
$$+ \int_0^\infty K_{01}(u,v;\underline{a}_4)\sigma(z,t;u)du\}$$
$$+ \tfrac{1}{2}\int_0^v K_{11}(u,v-u;a_4)n(z,t;u)n(z,t;v-u)du$$
$$+ [1-S(v;\underline{a}_2)][\int_0^v K_{10}(u,v-u;\underline{a}_4)$$
$$n(z,t;u)\sigma(z,t;v-u)du$$
$$+ \int_v^\infty \bar{u}_z(u;\underline{a}_1)\,\phi(u;\underline{a}_2)W(u,v)n(z,t;u)du] \quad (31)$$

$$\frac{\partial \sigma(z,t;v)}{\partial t} = [\bar{u}_z(v;\underline{a}_1)\lambda(v;\underline{a}_2)]n(z,t;v)$$
$$+ S(v;\underline{a}_2)[\int_0^v K_{10}(u,v-u;\underline{a}_4)$$
$$n(z,t;u)\sigma(z,t;v-u)du$$
$$+ \int_v^\infty \bar{u}_z(u;a_1)\,\phi(u;a_2)W(u,v)n(z,t;u)du]$$
$$- \sigma(z,t;v)\int_0^\infty K_{10}(u,v;\underline{a}_4)n(z,t;u)du \quad (32)$$

The physical meanings of the terms appearing in Equation (31) are as follows (from left to right): (1) rate of accumulation of moving v ganglia, (2) net efflux of v ganglia due to convection, (3) net efflux of v ganglia due to axial dispersion, (4) rate of loss of moving v ganglia due to stranding, fission, collision-coalescence with other moving ganglia and collision-coalescence with stranded ganglia, (5) rate of generation of moving v ganglia through collision-coalescence of appropriately sized smaller moving ganglia, (6) rate of generation of moving v ganglia through collision-coalescence of smaller moving ganglia with stranded ones, and through fission of larger ganglia.

The physical meanings of the terms of Equation (32) are (from

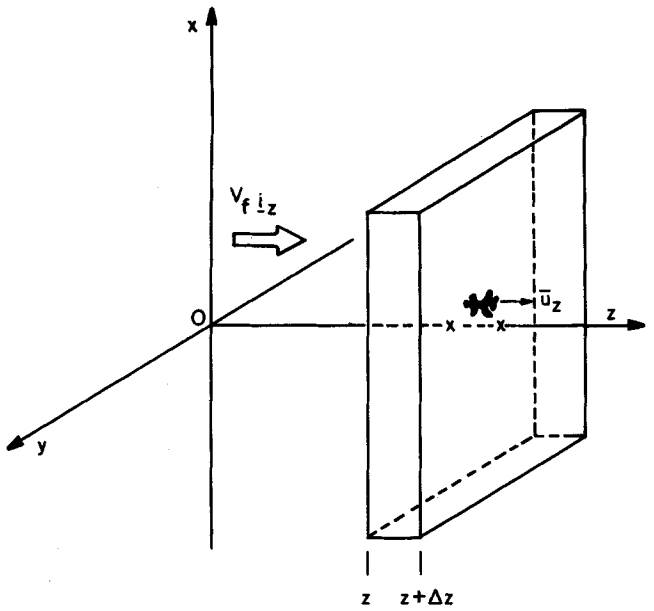

Figure 10. Control volume used in the analysis. Its thickness Δz is assumed large compared to the oil ganglia but small compared to the macroscopic dimensions of the reservoir.

*An interesting exception to this will be very small ganglia with diameters comparable to or less than the throat diameters of the porous medium. Such ganglia are carried by the moving continuous phase at significantly higher velocities than those of ganglia creeping along through rheons. They also can cause considerable increase of the pressure drop when they get strained at narrow throats. This last phenomenon is very similar to deep bed filtration with predominant straining (Payatakes, Brown and Tien, 1977; Tien and Payatakes, 1979). Formation of such small oil droplets is possible through snap-off from larger ganglia at narrow throats (Roof, 1970) and is deleterious to successful flooding, leading to formation of dilute oil-in-water emulsions. Here, we will assume that the conditions are such that this phenomenon does not take dimensions.

left to right): (1) rate of accumulation of stranded v ganglia, (2) rate of stranding of mobilized v ganglia, (3) rate of generation of stranded v ganglia through collision-coalescence of smaller ganglia, one of which is stranded, and through stranding of v ganglia formed by fission of larger ganglia, (4) rate of loss of stranded v ganglia by collision-coalescence with oncoming ganglia.

In the ganglion population balance equations

$$K_{ij}(u,v;\underline{a}_4) = [R_{ij}(u,v;\underline{a}_1) + D_{ij}(u,v;\underline{a}_1)]C_{ij}(u,v;\underline{a}_3) \quad (33)$$

are the collision-coalescence kernel functions.

Approximate expressions for the interception kernel functions R_{ij} and the dispersion kernel functions D_{ij} were derived in Payatakes, Flumerfelt and Ng (1978*a*) for sparse ganglion populations. It can be shown that the same expressions are also applicable to relatively dense ganglion populations:

$$R_{11}(u,v;\underline{a}_1) = \frac{\pi}{4}\left[\left(\frac{6u}{\pi}\right)^{1/3} + \left(\frac{6v}{\pi}\right)^{1/3}\right]^2 |\bar{u}_z(u;\underline{a}_1) - \bar{u}_z(v;\underline{a}_1)| \quad (34)$$

$$R_{10}(u,v;\underline{a}_1) = \frac{\pi}{4}\left[\left(\frac{6u}{\pi}\right)^{1/3} + \left(\frac{6v}{\pi}\right)^{1/3}\right]^2 \bar{u}_z(u;\underline{a}_1) \quad (35)$$

$$R_{01}(u,v;\underline{a}_1) = \frac{\pi}{4}\left[\left(\frac{6u}{\pi}\right)^{1/3} + \left(\frac{6v}{\pi}\right)^{1/3}\right]^2 \bar{u}_z(v;\underline{a}_1) \quad (36)$$

$$D_{11}(u,v;\underline{a}_1) = \pi\left[\left(\frac{6u}{\pi}\right)^{1/3} + \left(\frac{6v}{\pi}\right)^{1/3}\right]\left[D_x(u;\underline{a}_1) + D_x(v;\underline{a}_1)\right] \quad (37)$$

$$D_{10}(u,v;\underline{a}_1) = \pi\left[\left(\frac{6u}{\pi}\right)^{1/3} + \left(\frac{6v}{\pi}\right)^{1/3}\right]D_x(u;\underline{a}_1) \quad (38)$$

$$D_{01}(u,v;\underline{a}_1) = \pi\left[\left(\frac{6u}{\pi}\right)^{1/3} + \left(\frac{6v}{\pi}\right)^{1/3}\right]D_x(v;\underline{a}_1) \quad (39)$$

Ng and Payatakes showed that the stranding coefficient λ and the breakup coefficient ϕ can be obtained from the probabilities M, B and S pertaining to solitary ganglia:

$$\lambda = -\frac{S}{(1-M)}\frac{\ln M}{s_z} \quad (40)$$

$$\phi = -\frac{B}{(1-M)}\frac{\ln M}{s_z} \quad (41)$$

They also calculated the dispersion coefficients D_z and D_x as well as the breakup-mode probability density $W(u,v)$.

The system of Equations (31) and (32) can be integrated with appropriate initial and boundary conditions. If the axial dispersion term on the left-hand side of Equation (31) is neglected, the following boundary conditions can be used at the front of the flood:

$$\left.\begin{aligned} n &= F(z,v)[1-S(v;\underline{a}_2)]\left[1-\frac{\bar{u}_z(v;\underline{a}_1)}{V_f}\right] \\ \text{For } z &= V_f t, \quad t > 0: \\ \sigma &= F(z,v)\ S(v;\underline{a}_2) \end{aligned}\right\} \quad (42)$$

where $F(z,v)$ is a given function describing the initial spatial distribution of v ganglia for any value of v.

The parameter vectors $\underline{a}_1$ and $\underline{a}_2$ contain, among other parameters, the water saturation S_w. This, in turn, is given by

$$S_w = 1 - \frac{(m_1+\mu_1)}{\epsilon} \quad (43)$$

where m_1 and μ_1 are the first moments of n and σ, respectively:

$$m_1(z,t) = \int_0^\infty vn(z,t;v)dv, \quad \mu_1(z,t) = \int_0^\infty v\sigma(z,t;v)dv \quad (44)$$

This must be taken in account in integrating the population balance equations.

Fortunately, equations of this type appear quite frequently in particulate processes (sol or aerosol coagulation, crystallization, coalescence, living cell systems, etc.). Thus, numerous solution methods have appeared which can be applied to the problem at hand. Of these, collocation and the method of weighted residuals seem the most promising.

Limiting Case — No Coalescence

The importance of coalescence can be illustrated effectively by considering the hypothetical case when the oil ganglia are stabilized to the point where the probability of coalescence given a collision vanishes, $C_{ij}(u,v;\underline{a}_3) = 0$. To simplify matters, consider an initially monosized v ganglion population distributed uniformly in the range $z \geqq 0$, $[F(z,v) = \beta = \text{constant}]$. Neglecting the axial dispersion term from the left-hand side of Equation (31), and focusing on the v ganglia only, we get the simplified balance equations

$$\frac{\partial n(z,t;v)}{\partial t} + \bar{u}_z(v;\underline{a}_1)\frac{\partial n(z,t;v)}{\partial z} = -n(z,t;v)\ \bar{u}_z(v;\underline{a}_1)[\lambda(v;\underline{a}_2) + \phi(v;\underline{a}_2)]$$

$$\frac{\partial \sigma(z,t;v)}{\partial t} = \bar{u}_z(v;\underline{a}_1)\lambda(v;\underline{a}_2)n(z,t;v)$$

Introducing the new time variable

$$\tau = t - \frac{z}{\bar{u}_z(v;\underline{a}_1)} \quad (45)$$

we obtain the transformed v ganglion balance equations

$$\left(\frac{\partial n}{\partial z}\right)_\tau = -\bar{u}_z(\lambda+\phi)n \quad (46)$$

$$\left(\frac{\partial \sigma}{\partial \tau}\right)_z = \bar{u}_z\lambda n \quad (47)$$

These are to be integrated with the following initial and boundary conditions:

$$For\ z = -\tau\frac{V_f\bar{u}_z}{(V_f-\bar{u}_z)},\ \tau<0 : n = \frac{V_f\beta(1-S)}{(V_f-\bar{u}_z)},\ \sigma = \beta S \quad (48)$$

$$For\ \tau>0,\ z\geqq 0 : n = 0 \quad (49)$$

This system was solved in Payatakes, Flumerfelt and Ng (1978*a*) with the method of characteristics* to obtain

$$\frac{n}{\beta(1-S)} = \frac{V_f}{(V_f-\bar{u}_z)}\exp\left[-\frac{\bar{u}_z(\lambda+\phi)}{(V_f-\bar{u}_z)}(V_f t - z)\right] \quad \text{for } \bar{u}_z t < z \leqq V_f t \quad (50)$$

$$\frac{n}{\beta(1-S)} = \exp[-(\lambda+\phi)z] \quad \text{for } z = \bar{u}_z t \quad (51)$$

$$\frac{n}{\beta(1-S)} = 0 \quad \text{for } 0 \leqq z < \bar{u}_z t \quad (52)$$

$$\frac{\sigma-\beta S}{\beta(1-S)\left(\frac{\lambda}{\lambda+\phi}\right)} = 1 - \exp\left[-\frac{\bar{u}_z(\lambda+\phi)}{(V_f-\bar{u}_z)}(V_f t - z)\right] \quad \text{for } \bar{u}_z t \leqq z \leqq V_f t \quad (53)$$

$$\frac{\sigma-\beta S}{\beta(1-S)\left(\frac{\lambda}{\lambda+\phi}\right)} = 1 - \exp[-(\lambda+\phi)z] \quad \text{for } 0 \leqq z \leqq \bar{u}_z t \quad (54)$$

An upper bound for the microdisplacement efficiency under the present conditions can be obtained by assuming absence of ganglia breakup. This is due to the fact that if any daughter ganglia are produced, they have a higher probability of getting stranded. Hence, in order to study the best possible (actually unattainable) case, given the assumptions of this analysis, we set $\phi(v;\underline{a}_2) = 0$.

The flood in the absence of coagulation is quite ineffectual. Its main effect on the original population of v ganglia is to mobilize a number of them and transport them along various distances downstream, where they become stranded anew. The new trap positions are such that mobilization is not possible without improving the chemical flood conditions. As can be seen from the example in Figure 11, a traveling bulge is formed. Its front

*To avoid confusion, it must be noted that in the present work ϕ is defined slightly differently; it corresponds to $\phi\bar{u}_z$ in Payatakes et al. (1978).

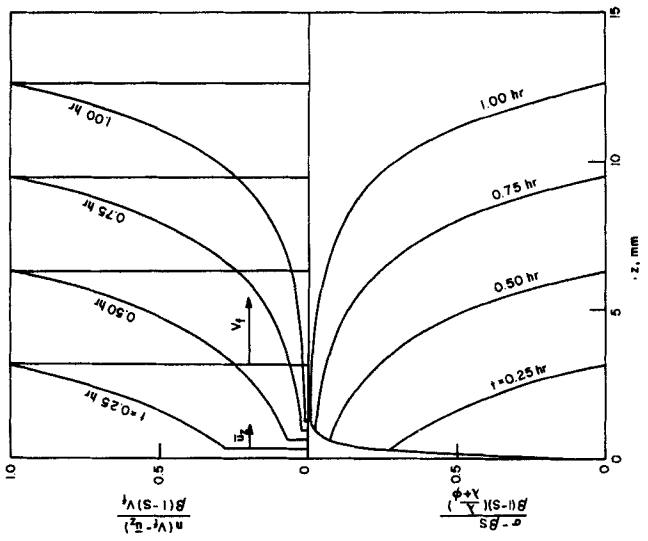

Figure 11. Traveling bulge of moving v ganglion concentration in the absence of coalescence. The corresponding stranded v ganglia concentration profile is also shown. Typical parameter values used in the calculation are: V_f = 3.5 μm/s, $\bar{u}_z$ = 0.35 μm/s, λ = 3 mm^{-1}, ϕ = 2 mm^{-1}.

moves with the front of the flood at velocity V_f, while its trailing edge moves with velocity u_z. Consequently, the bulge stretches rapidly with time. The value of $n(z,t;v)$ at the leading front is always $\beta[1-S(v;\underline{a}_2)]/(1-\bar{u}_z/V_f)$, whereas the value at the trailing edge decays as a negative exponential [Equation (50)].

The microdisplacement efficiency E_m, defined as the fraction of residual oil recovered at position $z=L$ at time t, is given by

$$\left.\begin{aligned} E_m(L,t) &= (Lv\beta)^{-1}\int_{L/V_f}^{t} vn(L,t;v)\,\bar{u}_z(v;\underline{a}_1)dt, \quad \text{for } t \leqq \frac{L}{\bar{u}_z} \\ E_m(L,t) &= (Lv\beta)^{-1}\int_{L/V_f}^{L/\bar{u}_z} vn(L,t;v)\,\bar{u}_z(v;\underline{a}_1)dt, \quad \text{for } t \geqq \frac{L}{\bar{u}_z} \end{aligned}\right\} \tag{55}$$

Maximum useful pore volumes correspond to $t = L/\bar{u}_z$. Beyond that point, no additional recovery can be expected without improving the flood conditions. Using Equations (50) and (55), we get

$$E_m(L,t) = \frac{(1-S)}{\lambda L}\left\{1-\exp\left[\frac{\bar{u}_z\lambda}{(V_f-\bar{u}_z)}(L-V_f t)\right]\right\} \text{ for } t \leqq \frac{L}{\bar{u}_z} \tag{56}$$

$$E_m(L,t) = \frac{(1-S)}{\lambda L}[1-\exp(-\lambda L)] \text{ for } t \geqq \frac{L}{\bar{u}_z}$$

Since L is of the order of 100 m and for typical capillary numbers λ is larger than 10 m^{-1} (Ng and Payatakes, 1980), we have $\lambda L > 10^3$, and therefore

$$E_m(L,t) \approx \frac{(1-S)}{\lambda L} < 10^{-3} \tag{57}$$

even for infinite pore volumes and discounting fission. Such a flood is very ineffective. This serves to underline the crucial importance of coalescence to successful chemical flooding.

The central role of coalescence is known to reservoir engineers both from laboratory and field tests. More recently, its role has been stressed and further explored by Wasan and his co-workers (Wasan et al., 1978, 1979). The present work makes possible the quantitative assessment of several dominant factors, including coalescence, on the dynamics of oil bank formation and attrition.

ACKNOWLEDGMENT

This work was performed under U.S. Department of Energy Grant No. E(40-1)-5075 and with support from Shell Oil Company and Marathon Oil Company. We thank Dr. James C. Melrose and Dr. Carl F. Brandner of Mobil Research and Development and Dr. Elmond Claridge of Shell Development Company for several valuable discussions during the formulation of this model.

NOTATION

a = maximum diameter of the periodically constricted tube corresponding to a given unit cell, Figure 1
a' = maximum diameter of a unit cell, Figure 1
$\underline{a}_1$, $\underline{a}_2$, $\underline{a}_3$, $\underline{a}_4$ = parameter vectors

$B(v;\underline{a}_2)$ = probability of breakup of a v ganglion per rheon
$C_{ij}(u,v;\underline{a}_3)$ = probability that a u ganglion and a v ganglion coming in contact will coalesce, before they are separated again by the flow; ij = 11 if both ganglia are moving, ij = 10 if only the u ganglion is moving and ij = 01 if only the v ganglion is moving
c_1, c_2, c_3 = constants defined by Equations (5) and (6)
$D_{ij}(u,v;\underline{a}_1)$ = collision kernel functions for dispersion; ij = 11 if both the u ganglion and the v ganglion are moving, ij = 10 if only the u ganglion is moving and ij = 01 if only the v ganglion is moving [Equations (37) to (39)]
$D_z(v;\underline{a}_1)$ and $D_x(v;\underline{a}_1)$ = axial and lateral dispersion coefficients for moving v ganglia
d = minimum diameter of a unit cell, Figure 1
d_c = effective constriction diameter
$d_{c,\max}$ = maximum experimental value of d_c
$d_{c,\min}$ = minimum experimental value of d_c
d_g = grain diameter
d_i = constriction diameter of the ith gate unit cell
$d_w(\phi_w)$ = diameter (function of ϕ_w) defined by Equation (29)
E_m = microdisplacement efficiency
$F(z,v)$ = function giving the spatial distribution of the number of v ganglia per unit volume for any value of v at the start of the chemical flood
f_{d_c} = constriction diameter frequency function
h = wavelength of the periodically constricted tube corresponding to a given unit cell, (length of extended unit cell), Figure 1
h' = length of unit cell, Figure 1
I = index of the gate unit cell through which the xeron takes place.
J_{dr} = drainage curvature
J_{imb} = imbibition curvature
J_{ow} = curvature of oil-water interface
K = index of the gate unit cell through which the hygron takes place
$K_{ij}(u,v;\underline{a}_4)$ = overall collision-coalescence kernel functions; ij = 11 if both the u ganglion and the v ganglion are moving, ij = 10 if only the u ganglion is moving and ij = 01 if only the v ganglion is moving
k = absolute (single phase) permeability
k_e = effective permeability to water
k_o, k_w = absolute permeabilities to oil and water, respectively
$k_{rw}=k_e/k_w$ = relative permeability to water
L = distance between injection and production points (here we neglect the radial nature of the flow pattern)
ℓ = length of periodicity of the porous medium
$M(v;\underline{a}_2)$ = probability that a v ganglion will undergo at least one rheon from its present position
$m_1(z,t)$ = first moment of $n(z,t;v)$
$N_{Ca}=\mu_w V_f/\gamma_{ow}$ = capillary number
N_p = number of pore chambers per unit volume
N_{Re} = Reynolds number of flow through a unit cell, Equation (16)

N_{uc} = number of unit cells (or constrictions) per unit volume

$n(z,t;v)\Delta v$ = number of moving v ganglia per unit reservoir volume

n_{th} = average number of satellite throats (constrictions) of an elemental void space

P = pressure; the subscripts o and w refer to the oil and water phase, respectively

q_{uc} = flow rate through a unit cell

$R_{ij}(u,v;\underline{a}_1)$ = collision kernel functions for interception; $ij = 11$ if both the u ganglion and the v ganglion are moving, $ij = 10$ if only the u ganglion is moving and $ij = 01$ if only the v ganglion is moving [Equations (34) to (36)]

r = radial coordinate in a unit cell, Figure 1

$r_w(z)$ = unit cell wall radius at axial position z

r_1^*, r_2^* = dimensionless minimum and maximum radii of the periodically constricted tube corresponding to an extended cell

$S(v;\underline{a}_2)$ = probability that a v ganglion introduced randomly in the porous medium will find itself stranded before a single rheon takes place; also, probability of stranding per rheon

S_w = water saturation

S_{wi} = irreducible water saturation

s_z = expected length of travel of the centroid of a v ganglion in the z direction per rheon

t = time measured from the initiation of the flood

$\vec{u}$ = superficial velocity vector

$\bar{u}_z(v;\underline{a}_1)$ = mean velocity of the centroids of v ganglia in the axial direction

V_f = superficial velocity of the aqueous phase

V_o = volume of oleic phase in the immediate neighborhood of a constriction

V_{uc} = unit cell volume

V_w = volume of water phase in the immediate neighborhood of a constriction

v_o = average velocity at the unit cell constriction

$W(u,v)\Delta v$ = probability that a u ganglion undergoing fission will produce two daughter ganglia, one of which is a v ganglion

x,y = Cartesian coordinates, Figure 10

z = axial coordinate in the unit cell, Figure 1; also, Cartesian coordinate in the direction of the flood, Figure 10

z^* = dimensionless axial coordinate in a unit cell

Greek Letters

α = angle between the axis of a unit cell and the macroscopic flow direction

$\gamma_{os}, \gamma_{ow}, \gamma_{ws}$ = interfacial tensions at the oil-solid, oil-water and water-solid interfaces, respectively

ΔP_h = pressure drop along an extended unit cell (single phase)

ΔP_h^* = dimensionless pressure drop along an extended unit cell

ΔP_1^* = dimensionless pressure drop along an extended unit cell at $N_{Re} = 1$, neglecting inertial effects, Figure 4

δ = distance between adjacent nodes of the tetrahedric lattice

ϵ = porosity

η = limiting value of ϕ_{ow}/ϕ_0 as $S_w \rightarrow 1$

θ = apparent contact angle as measured from the wetting phase

θ_{ij} = angle between the line connecting gate constriction i to gate constriction j and the macroscopic flow direction

κ = side of each elemental tetrahedron in the tetrahedric unit cell network

$\lambda(v;\underline{a}_2)$ = stranding coefficient

μ = dynamic viscosity

$\mu_1(z,t)$ = first moment of $\sigma(z,t;v)$

ν = kinematic viscosity

ρ = fluid density (single phase).

$\sigma(z,t;v)\Delta v$ = number of stranded v ganglia per unit reservoir volume.

τ = transformed time, Equation (45)

$\phi(v;\underline{a}_2)$ = breakup coefficient

ϕ_0, ϕ_w = number fraction of unit cells which are filled with oil or water, respectively

ϕ_{ow} = number fraction of unit cells that contain an oil-water interface (gate unit cells)

LITERATURE CITED

Everett, D. H., "Structure and Properties of Porous Materials," pp. 95-120, Academic Press, New York (1958).

Fatt, I., "The Network Model of Porous Media," (in three parts), *Petrol. Trans. Am. Inst. Mining Engrs.*, **207**, 144 (1956).

Fedkiw, P., and J. Newman, "Mass Transfer at High Peclet Numbers for Creeping Flow in a Packed Bed Reactor," *AIChE J.*, **23**, 255 (1977).

Heller, J. P., "The Drying Through the Top Surface of a Vertical Porous Column," *Soil Sci. Soc. Amer. Proc.*, **32**, 778 (1968).

Iczkowski, R. P., "Displacement of Liquids from Random Sphere Packings," *Ind. Eng. Chem. Fundamentals*, **7**,572 (1968).

Ksenzhek, O. S., "Capillary Equilibrium in Porous Media with Intersecting Pores," *Russ. J. Phys. Chem.*, **37**, 691 (1963).

Leverett, M. C., "Flow of Oil-Water Mixtures through Unconsolidated Sands," *Trans. AIME*, **132**, 149 (1939).

Leverett, M. C., "Capillary Behavior in Porous Solids," *Trans. AIME*, **142**, 152 (1941).

Melrose, J. C., "Wettability as Related to Capillary Action in Porous Media," *Soc. Petrol. Eng. J.*, **5**, 259 (1965).

Melrose, J. C., "Thermodynamics Aspects of Capillarity," *Ind. Eng. Chem.* **60**, No. 3, 53 (1968).

Melrose, J. C., and C. F. Brandner, "Role of Capillary Forces in Determining Microscopic Displacement Efficiency for Oil Recovery by Waterflooding," *Can. J. Petrol. Technol.*, **13**, No. 4, 54 (1974).

Miller, E. E., and R. D. Miller, "Physical Theory for Capillary Flow Phenomena," *J. Appl. Phys.*, **27**, 324 (1956).

Moore, T. F., and R. L. Slobod, "The Effect of Viscosity and Capillarity on the Displacement of Oil by Water," *Producers Monthly*, **20**, No. 10, 20 (1956).

Neira, M. A., and A. C. Payatakes, "Collocation Solution of Creeping Newtonian Flow Through Sinusoidal Tubes," *AIChE J.*, **25**, 725 (1979).

Ng, K. M., and A. C. Payatakes, "Stochastic Simulation of the Motion, Breakup and Stranding of Oil Ganglia in Water-Wet Granular Porous Media During Immiscible Displacement," *AIChE J.*, **26**, 419 (1980).

Ng, K. M., H. T. Davis and L. E. Scriven, "Visualization of Blob Mechanics in Flow Through Porous Media," *Chem. Eng. Sci.*, **33**, 1009 (1978).

Oh, S. G., and J. C. Slattery, "Interfacial Tension Required for Significant Displacement of Oil," *Proc. 2nd ERDA Symposium on Enhanced Oil and Gas Recovery*, Tulsa, Okla. (Sept., 1976).

Payatakes, A. C., D. H Brown and Chi Tien, "On the Transient Behavior of Deep Bed Filtration," AIChE 83rd National Meeting, Houston, Tex. (Mar. 20-24, 1977).

Payatakes, A. C., R. W. Flumerfelt and K. M. Ng, "Model of Isotropic Granular Porous Media for the Simulation of Oil Ganglia Motion, Partition and Coalescence During Immiscible Displacement," AIChE 70th Annual Meeting, New York (Nov. 13-17, 1977).

Payatakes, A. C., R. W. Flumerfelt and K. M. Ng, "On the Dynamics of Oil Ganglia Populations During Immiscible Displacement," AIChE 84th National Meeting, Atlanta, Ga. (Feb. 26-Mar. 1, 1978*a*).

Payatakes, A. C., R. W. Flumerfelt and K. M. Ng, "Oil Ganglia Dynamics During Immiscible Displacement. Effects of Interfacial Properties," *Proc. 4th DOE Symposium on Enhanced Oil and Gas Recovery*, Tulsa, Okla. (Aug. 29-31, 1978*b*).

Payatakes, A. C., and M. A. Neira, "Model of the Constricted Unit Cell Type for Isotropic Granular Porous Media," *AIChE J.*, **23**, 922 (1977).

Payatakes, A. C., Chi Tien and R. M. Turian, "A New Model for Granular Porous Media-Part I. Model Formulation," *ibid.*, **19**, 58 (1973*a*).

Payatakes, A. C., Chi Tien and R. M. Turian, "A New Model for Granular Porous Media -Part II. Numerical Solution of Steady State Incompressible Newtonian Flow Through Periodically Constricted Tubes," *ibid.*, **19**, 67 (1973*b*).

Reisberg, J., and T. Doscher, "Interfacial Phenomena in Crude Oil-Water Systems," *Producers Monthly*, **21**, No. 1, 43 (1956).

Roof, J. C., "Snap-off of Droplets in Water Wet Pores," *Soc. Petrol. Eng. J.*, **10**, 85 (1970).

Slattery, J. C., "Interfacial Effects in the Entrapment and Displacement of Residual Oil," *AIChE J.*, **20**, 1145 (1974).
Stegemeier, G. L., "Mechanisms of Entrapment and Mobilization of Oil in Porous Media," AIChE 81st Nat. Meeting, Kansas City, Mo. (Apr. 1976).
Tien, Chi and A. C. Payatakes, "Advances in Deep Bed Filtration, *AIChE J.*, **25**, 737 (1979).
van Brakel, J., "Pore Space Models for Transport Phenomena in Porous Media. Review and Evaluation with Special Emphasis on Capillary Liquid Transport," *Powder Technol.*, **11**, 205 (1975).
Wasan, D. T., K. Sampath, J. J. McNamara, et al., "The Mechanism of Oil Bank Formation, Coalescence in Porous Media and Emulsion Stability," *Proc. 4th DOE Symposium on Enhanced Oil and Gas Recovery*, Tulsa, Okla. (Aug. 29-31, 1978).
Wasan, D. T., J. J. McNamara, S. M. Shah, et al., "The Role of Coalescence Phenomena and Interfacial Rheological Properties in Enhanced Oil Recovery: An Overview," *J. of Rheology* **23**, No. 2, 181 (1979).

Manuscript received January 17, 1979; revision received October 4, and accepted October 11, 1979.

Dendritic Deposition of Aerosols by Convective Brownian Diffusion for Small, Intermediate and High Particle Knudsen Numbers

A. C. PAYATAKES
and
L. GRADOŃ
Chemical Engineering Department
University of Houston
Houston, Texas 77004

When an aerocolloidal suspension flows through a fibrous filter, particles deposit on the fibers and form dendrites. Similar phenomena are observed with collectors other than fibers, provided that the characteristic dimension of the collector does not exceed that of the particles by more than one to two orders of magnitude. This deposition pattern leads to marked increases in capture efficiency and pressure drop, as particles accumulate within the filter. In previous publications, theoretical models of this process were developed for the cases of deposition by interception alone and of deposition by combined inertial impaction and interception. Consequently, those works apply to aerosol particles with diameters of 1 μm or larger. Here we extend the model to the case of submicron particles, where the main transport mechanism is Brownian diffusion. To keep things specific, we consider fine fibers as collectors, but the model can be easily converted to other geometries. We present solutions for the cases of nonslip flow around the fiber and nonslip, slip and free molecular flow around particles. Unlike deposition by inertial impaction and/or interception, convective Brownian diffusion forms dendrites over the entire fiber surface.

SCOPE

Aerosol filtration in fibrous mats is one of the most efficient methods of solid-gas separation, especially in the case of submicron particles. Fibrous filters are compact, provide excellent capture efficiency and present minimal resistance to flow. For given pressure drop, the flow rate through a fibrous filter is several times higher than that through a fabric filter of equal area, without sacrifice in capture efficiency or danger of blinding. Their main drawback seems to be that in situ cleaning is usually difficult. Hence, most industrial applications are still confined to cases where high efficiency is demanded and where the use of disposable filter elements is practical (clean rooms, emergency filtration systems for radioactive aerosols, absolutely clean air supply for aseptic fermentation processes, respiration masks, automobile air intake and exhaust filters, etc.).

The pattern of particle deposition in a fibrous filter is highly complex and intrinsically connected with the efficiency, loading capacity and permeability of the system. Therefore, rational design, optimization, operation, troubleshooting and innovation require intimate understanding and reliable analysis of the deposition process and its effects on the system variables. During an initial period, aerosol particles deposit on the collector surfaces, forming chainlike agglomerates. This phenomenon and its consequences have been analyzed for the case of particles larger than 1 μm in Payatakes (1977) assuming deposition by interception alone, and in Payatakes and Gradoń (1979) for deposition by combined inertial impaction and interception. In the present work, we deal with the important case of submicron particles, where the dominant transport mechanism is convective Brownian diffusion.

Dr. Leon Gradoń is on leave from the Chemical Engineering Department of the Technical University of Warsaw, Poland.

0001-1541-80-3516-0443-$01.35.